2. **Penalty formulation with flexible bodies**: This methodology is conceptually similar to the previous approach. In this formulation though, the single bodies are considered as flexible. The contact behavior is not anymore solely defined by the force law but it is directly included in the material, geometric and kinematic properties of the flexible bodies. The continuous force law might still have the form of a power law based on Hertz theory, e.g. in case the flexible body representation does not inherently account for local non-linearities in the contact region. Advantages and disadvantages are similar to the previous approach even though more complex in implementation, numerically less efficient but more accurate. As underlined in [11] the method might suffer from ill-conditioning due to the high value of penalty parameter needed for the correct contact constraints enforcement. Since this is the method adopted in this work, more details are presented in a later section.
3. **Lagrangian approach**: This approach mainly consists of converting the inequality constraints related to the contact kinematic problem into equality constraints that can be treated with the Lagrange multipliers approach. Even though mathematically sound, this method is often numerically inefficient due to the higher number of variables and indefinite structure of the resulting equations of motion [11].
4. **Augmented Lagrangian approach**: This approach combines the main ideas of the two previous methods and can be interpreted as an interative penalty method [12]. As noted in [11] the method keeps the number of variables reduced leading to algorithms of similar complexity with respect to penalty formulations while providing increased robustness.
5. **Linear Complementarity Problem (LCP)**: This non-smooth contact approach makes use of results well known in optimization theory, to impose directly the inequality constraints derived from contact kinematics. Discontinuous events like detachment conditions, stick-slip, and impacts can be treated. The approach allows for the simulation of contact between rigid bodies [4] and flexible bodies [13]. The main drawbacks include the difficulty of extending the approach to 3D frictional contact for which polygonalization of the friction cones has to be used, the restrictions of accounting for friction models different from Coulomb and the numerical challenges arising when multiple contacts are present [2].
6. **Time stepping algorithms**: As in the case of LCP, this approach treats the contact kinematics by enforcing the correct contact inequality constraints. The main difference with respect to standard LCP lies in the fact that the contact problem is handled by means of a difference-equation that can be used for a convergence proof of multiple impact problems [2]. These formulations are mathematically sound and accurate but the solution of multiple inequalities at each iteration step makes them numerically intensive and of more complex implementation.
7. **Combined FE-surface integral method**: This approach uses a combined FE-surface integral method to evaluate a variable stiffness matrix that is computed at each time step by solving a quasi-static LCP [5, 14]. The contact kinematics is idealized as a point or line contact for the stiffness computation and the equations of motion can then be time integrated by using one of several different approaches. Non-linearities arising in the contact zone can be properly modeled to retrieve meaningful stress and strain fields and the amount of finite elements in the contact zone can be significantly reduced due to the surface integral formulation. Nonetheless, the method is numerically expensive and of more difficult implementation as compared to penalty formulations.

### *2.2. Model order reduction in flexible multibody systems*

In the frequent case when deformations remain small, the elastic forces can be approximated as linear with respect to the motion of a reference frame, often referred to as Floating Frame of

Reference (FFR), see e.g. [15]. Linear FE models can be directly included in flexible multibody codes using the FFR formulation. The number of DOF present in these models is usually very large so that the deformation of each body is approximated by using a reduced set of shape vectors instead of the complete set of nodal coordinates. The choice of the vector set used to represent the body flexibility frequently distinguishes one MOR technique from another. One of the main challenges encountered in contact between flexible bodies relates to the difficulty of applying MOR techniques due to the intrinsic variable MIMO characteristic of the problem. A brief review of the most commonly used MOR techniques is presented, contextualizing their possible use for contact and impact modeling.

1. **Modal**: This well established approach consists of projecting the original flexible DOF on a subspace spanned by a certain set of eigenvectors or eigenmodes. These have to fulfill the geometric boundary conditions (BC) imposed by the adopted floating frame. The main drawback of simple modal approaches is their inability to satisfy exactly the dynamic BC imposed by externally applied loads. In gear simulations for example, these BC are multiple and continuously varying, see e.g. [16, 17]. This results in a slow convergence of the reduced model towards the original FE representation. The main advantage of this method, especially for the case of systems with variable topology and more specifically for gear contact, is its independence with respect to the MIMO characteristics of the system. For this reason, e.g., in [18] this methodology was successfully applied to gear contact problems.
2. **Modal with static augmentation**: This projection method is conceptually similar to the modal approach. The main difference lies in the additional use of static shape vectors, also referred to as static vectors to augment the subspace spanned by the eigenvectors. A comprehensive overview of different ways for static augmentation can be found in [19]. The main advantage lies in the fulfillment of the dynamic BC and in the fact that static solutions can be obtained with the same level of accuracy of the underlying FE model. One main drawback appears when large flexible interfaces or variable topologies are considered. A large number of static shapes needs to be included jeopardizing the numerical efficiency of this MOR scheme. However, as it is underlined in [17], the inclusion of static shape vectors improves the solution accuracy and allows for superior displacement and stress evaluation. For this reason, this approach is used in this work, showing how gear contact can highly benefit from a proper use of static augmentation. Moreover it is shown how the efficiency limitations can be improved by selecting the proper static shape vectors and applying the SMS methodology [8].
3. **Moment matching**: This methodology is often used when the input-output characteristics of the system is of high importance and it is usually realized by projection onto a Krylov subspace. The reduced system approximates the frequency response function of the underlying FE model at discrete frequencies [16]. The main advantages of this method are the ability of producing accurate results in a specific frequency range and the possibility of automated error control [20]. However the stability of the reduced model in not necessarily preserved for second order systems [20]. Moreover, as the previous method, it is often practically unfeasible to apply it as such to systems with variable topology and especially not to gear contact due to their variable MIMO characteristics.
4. **Gramian matrix**: The main underlying idea consists of removing some of the states that do not contribute to the system Input-Output (I/O) behavior. This is done by exploiting the characteristics of the controllability and observability Gramian matrices. The main advantages are the accuracy in a specified frequency range, the stability preserving characteristics and the

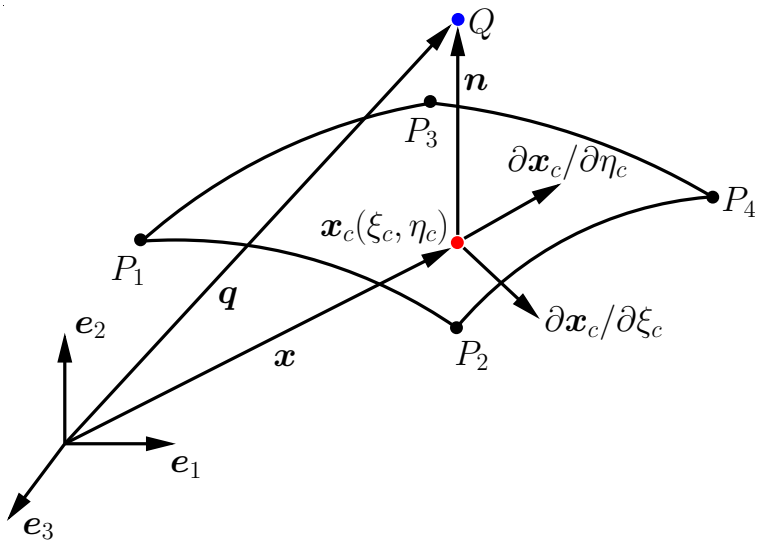


Figure 1: Node-to-surface contact element

possibility of having a-priori error bounds [20]. Unfortunately since this method also depends on the MIMO characteristics of the system, it is not ideal for simulation of contact problems.

To summarize, in this work the modal method with static augmentation is adopted, mainly to highlight the desirable characteristics of this approach and the necessity of static vectors inclusion for more accurate results. It will be shown that this method can be extended to gear contact simulation despite the large number of static shape vectors originally needed.

## 3. Static modes switching for gear contact

### *3.1. Contact formulation*

The contact formulation adopted in this work belongs to the category of penalty formulations. For more details the interested reader is referred to [6, 18]. Here a brief review of the approach is presented. The implemented scheme focuses on frictionless normal contact between flexible bodies. For an accurate description of the gear teeth geometry, especially in the contact zone, a 3D contact formulation is necessary. Several contact elements have been described in literature [6]. In this work the node-to-surface element described in Fig.1 is adopted. This element involves the distinction between a master and a slave body. The nodes of the slave body are checked for penetration within the master elements. The points $P_1$ to $P_4$ describe a master element with which the slave node Q might be in contact. Without loss of generality and following the modeling approach adopted in this work, the gear FE model is composed of eight nodes hexahedral elements for which the flexible deformation **x** can be described by linear shape functions. Following the displacement field and shape function definition for the surface of each hexahedral element

$$\mathbf{x}(\xi,\eta) = \frac{1}{4}\sum_{i=1}^{4}(1+\xi_i\xi)\,(1+\eta_i\eta)\,\mathbf{z}_{F,i}, \quad \xi_i,\eta_i \in [\pm 1], \quad -1 \le \xi,\eta \le 1 \tag{1}$$

where $\xi_i$ and $\eta_i$ define the element boundaries and $\mathbf{z}_{F,i}$ are the nodal coordinates of the corner nodes. The essential kinematic quantity for the contact force computation is the penetration of the node Q within the master element. To solve for the projected distance of Q on the master element, the conditions

$$\frac{\partial \mathbf{x}}{\partial \xi}\left[\mathbf{q}-\mathbf{x}(\xi,\eta)\right] = 0, \quad \frac{\partial \mathbf{x}}{\partial \eta}\left[\mathbf{q}-\mathbf{x}(\xi,\eta)\right] = 0 \tag{2}$$

should be imposed between the penetration vector and the master surface derivatives. See Fig.1 for a visual explanation of the symbols. These non-linear problems can be iteratively solved for $\xi_c$ and $\eta_c$ that in turn give the contact point $x_c$. At this stage the penetration value and the normal vector $\mathbf{n}$ to the master surface can be calculated explicitly. In case the node Q lies exactly on a master element edge or node, special precautions should be taken [6]. If the penetration $g_n$>0, then the contact is not taking place. If instead $g_n \le 0$, then a contact event is detected and the force $\mathbf{f}_S = \mathbf{n}(\xi_c,\eta_c)\,f_S$ can be applied to the slave node and distributed to the four master element nodes

$$\mathbf{f}_{M,1} = -\frac{1}{4}(1+\xi_c)(1+\eta_c)\,f_S\,\mathbf{n}, \quad \mathbf{f}_{M,2} = -\frac{1}{4}(1-\xi_c)(1+\eta_c)\,f_S\,\mathbf{n}, \tag{3}$$

$$\mathbf{f}_{M,3} = -\frac{1}{4}(1-\xi_c)(1-\eta_c)\,f_S\,\mathbf{n}, \quad \mathbf{f}_{M,4} = -\frac{1}{4}(1+\xi_c)(1-\eta_c)\,f_S\,\mathbf{n}. \tag{4}$$

The choice which of the two flexible bodies is the master body and which one is the slave is arbitrary and the results might be slightly affected by this choice. A better approach, adopted in this work, see [18, 21], is the use of a two-pass algorithm in which the two contacting bodies are alternatively chosen as master or slave and the reaction force is the average based on a user parameter $w_f \in [0;1]$

$$\mathbf{f}_S = w_f\mathbf{f}_S^{(MS)} + \left(1-w_f\right)\mathbf{f}_S^{(SM)}, \tag{5}$$

$$\mathbf{f}_{M,i} = w_f\mathbf{f}_{M,i}^{(MS)} + \left(1-w_f\right)\mathbf{f}_{M,i}^{(SM)}, \quad i = 1,2,3,4. \tag{6}$$

Finally the nodal slave load is defined by the penetration and the user defined penalty factor $c_p$

$$f_S = c_p\,|g_n(\xi_c,\eta_c)|\,, \quad g_n \le 0. \tag{7}$$

The parameter $c_p$ deserves a particular discussion, being the discriminant between an accurate and a meaningless simulation. A physical interpretation of this parameter is to consider it as a stiffness term that is placed in series with the local stiffness given by the FE model in the contact zone. It is well known that the exact contact constraints are enforced exactly only in the limit of $c_p \to \infty$ [6]. Obviously by setting this parameter to a very high numerical value, the stiffness of the numerical contact problem increases drastically and ill-conditioning is unavoidable. One has to accept a slight violation of the contact constraint, and set the $c_p$ parameter as high as possible, e.g. two or three orders of magnitude higher than the stiffness of the contacting gear teeth. It will be shown by means of numerical results that the inclusion of static shape vectors, that are able to properly model the local teeth flexibility, decreases significantly the contacting teeth stiffness yielding a problem that is numerically better conditioned. This allows in turn to choose a higher

penalty factor so that the contact constraints are more accurately enforced and the tooth local displacement field is better approximated.

The contact search strategy is described in [18] and is based on a two step approach. First a coarse collision detection allows determining the teeth pairs that are most likely in contact. Secondly, the possible nodes in contact on each flank are checked for penetration. The algorithm is implemented such that the memory usage needed for this computationally quite extensive task is considerably reduced. This modeling approach was also experimentally validated, see e.g. [22].

### *3.2. Static modes switching*

The SMS procedure is outlined in the following. For more details related to the full procedure, the interested reader is referred to [8] and [9]. The creation of a reduction space suitable for SMS application can be summarized in three main steps. This space is composed by a certain number of dynamically responding modes (usually the first eigenmodes of the flexible body) and a set of statically responding modes (as a preferred choice residual attachment modes can be used) that have a one-to-one relation with each I/O point of the system. This means that each single statically responding mode can be uniquely related to a single nodal load in a defined direction. The one-to-one relation is necessary to exploit some physical characteristics of this mode or vector set that will be discussed in detail later. The three pre-processing steps are as follows:

**Step 1**: Selection of a set of linearly independent vectors that reduce the number of DOF of a flexible body and, that is able to accurately represent the static behavior and the dynamic frequency response behavior of the system. One often good choice for this vector set is the inclusion of all the eigenmodes in the frequency range of interest and all the attachment modes that are necessary to accurately define the static deformation for each of the possible I/O points in which the system will be loaded. Equation (8) shows the general approach and in parallel the specific approach adopted in this work. To clarify this definition further, the general case shows how the first of the pre-processing steps is perfomed starting from a general vector set. The particular case present in more details the same pre-processing step when the starting vector set is composed by eigenmodes and all the possible attachment modes. The superscript $g$ stands for general case, $p$ for particular, the subscript $m$ stands for eigenmodes, $a$ for attachment modes, $f$ for flexible and $FE$ for finite elements

$$\begin{array}{ll} \text{general case} & \text{particular case} \\ \boldsymbol{\Psi}^g \mathbf{q}^g \cong \mathbf{x}, & \boldsymbol{\Psi}^p \mathbf{q}^p = \left[\boldsymbol{\Psi}^p_m \boldsymbol{\Psi}^p_a\right] \begin{bmatrix} \mathbf{q}^p_m \\ \mathbf{q}^p_a \end{bmatrix} \cong \mathbf{x}. \end{array} \tag{8}$$

In Eq. (8), $\mathbf{x}$ represents the original FE nodal displacement field that is approximated by means of a reduced number of flexible coordinates or Modal Participation Factors (MPF) $\mathbf{q}$ pro-

jected onto the vector space spanned by $\boldsymbol{\Psi}$

general case | particular case

$$\boldsymbol{M}_{ff}^{g} = \boldsymbol{\Psi}^{gT}\boldsymbol{M}_{FE}\boldsymbol{\Psi}^{g}, \qquad \boldsymbol{M}_{ff}^{p} = \begin{bmatrix} \boldsymbol{M}_{ff}^{mm} & \boldsymbol{M}_{ff}^{am} \\ \boldsymbol{M}_{ff}^{ma} & \boldsymbol{M}_{ff}^{aa} \end{bmatrix} = \boldsymbol{\Psi}^{pT}\boldsymbol{M}_{FE}\boldsymbol{\Psi}^{p},$$

$$\boldsymbol{K}_{ff}^{g} = \boldsymbol{\Psi}^{gT}\boldsymbol{K}_{FE}\boldsymbol{\Psi}^{g}, \qquad \boldsymbol{K}_{ff}^{p} = \begin{bmatrix} \boldsymbol{K}_{ff}^{mm} & \boldsymbol{K}_{ff}^{am} \\ \boldsymbol{K}_{ff}^{ma} & \boldsymbol{K}_{ff}^{aa} \end{bmatrix} = \boldsymbol{\Psi}^{pT}\boldsymbol{K}_{FE}\boldsymbol{\Psi}^{p}, \tag{9}$$

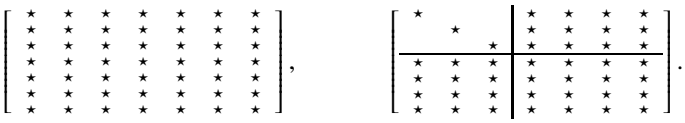

Equation (9) shows the reduced mass $\boldsymbol{M}_{ff}$ and stiffness $\boldsymbol{K}_{ff}$ matrices and the difference in sparsity patterns between different initial choices for the reduction space. In the particular case adopted in this work, the upper left block of the reduced matrices is diagonal due to the choice of eigenmodes to represent the dynamic behavior of the body.

**Step 2**: After the model is reduced, a mass orthonormalization procedure should be performed. In the particular case that the suggested set of vectors is chosen, the orthonormalization process does not modify the shape of the eigenmodes but changes the shape of the attachment modes. The space spanned by all the orthonormalized attachment modes represents only the part of static contribution of the attachment modes that is residual to the eigenmodes. At this point diagonally reduced mass and stiffness matrices are obtained. Equations (10) and (11) show the mass orthonormalization procedure performed by generalized eigenvalue decomposition of the pencil $(\boldsymbol{K}_{ff}, \boldsymbol{M}_{ff})$

$$\left(-\hat{\boldsymbol{\Lambda}}\boldsymbol{M}_{ff} + \boldsymbol{K}_{ff}\right)\hat{\boldsymbol{\Psi}} = \boldsymbol{0}, \tag{10}$$

$$\boldsymbol{M}_{ff}^{ortho} = \hat{\boldsymbol{\Psi}}^{T}\boldsymbol{M}_{ff}\hat{\boldsymbol{\Psi}}, \quad \boldsymbol{K}_{ff}^{ortho} = \hat{\boldsymbol{\Psi}}^{T}\boldsymbol{K}_{ff}\hat{\boldsymbol{\Psi}}. \tag{11}$$

Here $\hat{\boldsymbol{\Lambda}}$ is the eigenvalues matrix, $\boldsymbol{M}_{ff}^{ortho}$ is the identity mass matrix and $\boldsymbol{K}_{ff}^{ortho} = \hat{\boldsymbol{\Lambda}}\boldsymbol{M}_{ff}^{ortho} = \hat{\boldsymbol{\Lambda}}$ is the the orthogonalized diagonal reduced stiffness matrix of the flexible body. Important is to notice that $\hat{\boldsymbol{\Psi}}$ spans the same space as $\boldsymbol{\Psi}$ and only a change of basis is performed. Moreover, following the notation in Eq. 8, by performing the operation in Eq. 10 the columns of $\boldsymbol{\Psi}_{a}^{p}$ are projected onto a space that is orthogonal to the column space of $\boldsymbol{\Psi}_{m}^{p}$.

**Step 3**: Based on the frequency range of interest only a few vectors are chosen as dynamically responding and the rest to respond quasi-statically, see Eq. (12). If the suggested set of vectors is adopted, the eigenmodes are chosen to respond dynamically while the residual attachment vector space is chosen to respond statically

$$\boldsymbol{M}_{ff}^{ortho} = \begin{bmatrix} \boldsymbol{M}_{dyn} & 0 \\ 0 & \boldsymbol{M}_{stat} \end{bmatrix}, \quad \boldsymbol{K}_{ff}^{ortho} = \begin{bmatrix} \boldsymbol{K}_{dyn} & 0 \\ 0 & \boldsymbol{K}_{stat} \end{bmatrix}. \tag{12}$$

Comments on the amount of eigenmodes to be included for an accurate simulation will be presented in section 4. At this point it is possible to apply independently a unit load to each of the possible I/O points of the flexible body and to compute vector shapes that represent the residual

static deformation of the flexible body with the same degree of accuracy as the original model, see

$$\boldsymbol{K}_{stat}\hat{\boldsymbol{\Psi}}^{j}_{res} = \boldsymbol{f}^{proj,j}_{ext} \quad , \quad j = 1, 2, ..., n\, I/O\ points. \tag{13}$$

Here, $\boldsymbol{f}^{proj,j}_{ext}$ represents a load vector for each of the I/O points of the flexible body, projected onto the mass orthogonal subspace spanned by the attachment modes only. The equation is solved separately for each of the I/O points to obtain the residual vector space $\hat{\boldsymbol{\Psi}}_{res}$ that is used to obtain the mass $\boldsymbol{M}_{res}$ and stiffness $\boldsymbol{K}_{res}$ matrices

$$\boldsymbol{M}_{res} = \hat{\boldsymbol{\Psi}}^{T}_{res}\boldsymbol{M}_{stat}\hat{\boldsymbol{\Psi}}_{res}, \quad \boldsymbol{K}_{res} = \hat{\boldsymbol{\Psi}}^{T}_{res}\boldsymbol{K}_{stat}\hat{\boldsymbol{\Psi}}_{res}. \tag{14}$$

It has to be noticed that the procedure in general can be adopted by using any starting vector set. If the suggested base is used, the final space consists of eigenmodes and residual attachment modes. This set has the property of satisfying the dynamic and geometric boundary conditions related to the floating frame definition, constraints and external forces. A comprehensive investigation on different mode sets with the same characteristics can be found in [19] and [17]. In summary, the flexible body is reduced according to

$$\hat{\boldsymbol{\Psi}}_{red} = \begin{bmatrix} \hat{\boldsymbol{\Psi}}_{dyn} & \hat{\boldsymbol{\Psi}}_{res} \end{bmatrix}, \hat{\boldsymbol{q}}_{red} = \begin{bmatrix} \hat{\boldsymbol{q}}_{dyn} & \hat{\boldsymbol{q}}_{res} \end{bmatrix}, \tag{15}$$

$$\boldsymbol{M}_{red} = \begin{bmatrix} \boldsymbol{M}_{dyn} & 0 \\ 0 & \boldsymbol{M}_{res} \end{bmatrix} = \hat{\boldsymbol{\Psi}}^{T}_{red}\boldsymbol{M}^{ortho}_{ff}\hat{\boldsymbol{\Psi}}_{red}, \tag{16}$$

$$\boldsymbol{K}_{red} = \begin{bmatrix} \boldsymbol{K}_{dyn} & 0 \\ 0 & \boldsymbol{K}_{res} \end{bmatrix} = \hat{\boldsymbol{\Psi}}^{T}_{red}\boldsymbol{K}^{ortho}_{ff}\hat{\boldsymbol{\Psi}}_{red}, \tag{17}$$

$$\boldsymbol{x} \cong \boldsymbol{\Psi}^{T}\hat{\boldsymbol{\Psi}}^{T}\hat{\boldsymbol{\Psi}}^{T}_{red}\hat{\boldsymbol{q}}_{red} = \begin{bmatrix} \boldsymbol{\Psi}_{dyn} & \boldsymbol{\Psi}_{res} \end{bmatrix}^{T}\hat{\boldsymbol{q}}_{red}. \tag{18}$$

Here, $\boldsymbol{M}_{dyn}$ and $\boldsymbol{K}_{dyn}$ are the diagonal mass and stiffness sub-matrices that will respond dynamically in the equations of motion and are obtained by pre and post multiplication with the eigenmodes $\hat{\boldsymbol{\Psi}}_{dyn}$ each of which is associated with the generalized coordinates $\hat{\boldsymbol{q}}_{dyn}$. On the contrary $\boldsymbol{M}_{res}$ and $\boldsymbol{K}_{res}$ are the full mass and stiffness sub-matrices that will respond quasi statically in the equations of motion and are obtained by pre and post multiplication with the residual attachment modes $\hat{\boldsymbol{\Psi}}_{res}$ each of which is associated with the generalized coordinates $\hat{\boldsymbol{q}}_{res}$.

A particularly desirable characteristic of the residual attachment modes $\boldsymbol{\Psi}_{res}$ can be exploited during simulation. If the system is externally loaded in a few DOF, only the $\boldsymbol{\Psi}_{res}$ corresponding to the loaded DOF will be contributing to the system response. In practice, besides external loads, the residual attachment modes $\boldsymbol{\Psi}_{res}$ can still be excited by inertia coupling, through quadratic velocity terms and constraints present in the equations of motion. To limit the importance of these

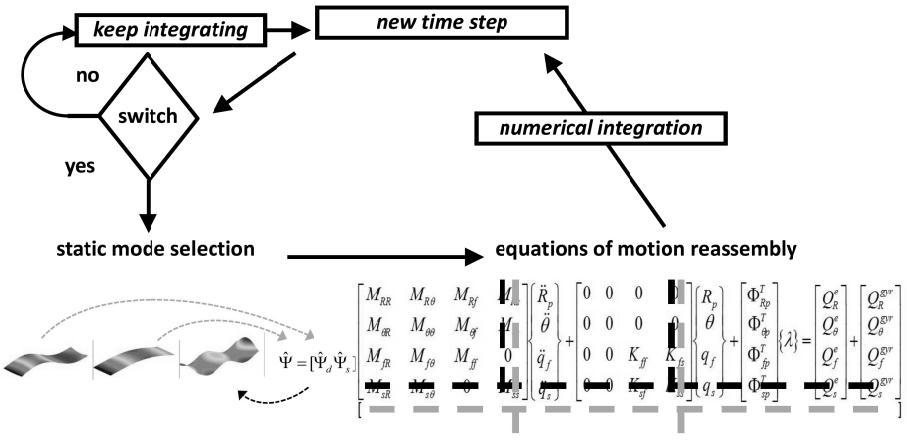


Figure 2: Static modes switching strategy

terms, the use of the Buckens frame or a tangent frame locked at the center of gravity, together with the SMS technique is advised. It is an approximation, validated by numerical experiments presented in [8] and further confirmed in the following sections, to assume these weak couplings to be negligible with respect to the excitation given by external loads. Under this assumption, if a load acting on a certain DOF is removed, the MPF of the corresponding residual attachment mode $\mathbf{\Psi}_{res}$ will damp out fast because of its intrinsic high frequency nature that makes it more sensitive to damping in the physical system. Acknowledging these effects, at a certain moment in time, only the dynamically responding modes and the residual attachment modes corresponding to the actual load acting on the system enrich the modal base significantly and should be included in the system representation. A single sentence can be used to summarize the principle behind SMS: If a DOF is no longer loaded, the corresponding $\mathbf{\Psi}_{res}$ can be excluded from the simulation and vice versa when a new DOF is loaded, the corresponding $\mathbf{\Psi}_{res}$ should be included. Practically this can be done by reassembling, during computation, the required matrices in the equations of motion, Fig.2. Numerically speaking, the on-line inclusion/exclusion of a specific residual attachment mode in the equations of motion introduces small amplitude impulses into the system. Up to now this problem was treated by exploiting the desirable numerical damping characteristics of the generalized-$\alpha$ solver and by adopting some particular projection techniques. In this work an explicit Runge-Kutta scheme of order four is used. This scheme does not present any numerical damping and the SMS assumptions are tested making use of proportional damping only. Even if the above outlined procedure is general and independent with respect to the original vector set adopted for the reduction of the flexible body, in this work the following vector set, complying with geometrical and dynamic boundary conditions is used: eigenmodes computed by constraining to zero displacement the bore DOF and so the center of gravity and keeping all the teeth flanks in free conditions are chosen to respond dynamically (fixed-free eigenmodes) while

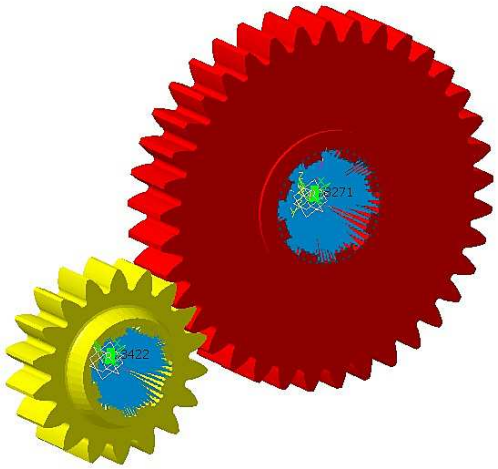

Figure 3: View of the gear pair example adopted for the numerical simulations

residual attachment modes are chosen to respond quasi-statically. The next sections show the high importance covered by the introduction of the proper residual attachment modes in terms of local flexible deformation during the meshing process of two gears.

## 4. Numerical results

### *4.1. Model description*

The model used for numerical validation is composed by the two spur gears represented in Fig.3. The small gear is named *Ritzel* and has 18 teeth while the larger is referred to as *Grossrad* and has 37 teeth. For the numerical validation, only one teeth pair is considered to be in contact at each instant during the time simulation. The two gears are modelled as flexible bodies and present a single rigid DOF each, namely the axial rotation. The two gears are finely meshed, especially in the vicinity of the possible contact zone by using hexahedral linear elements with eight nodes, see Fig.4. The floating frame connected to each of the gears is rigidly attached to a node positioned at the center of gravity. This frame is in turn connected to all the nodes present on the bore surfaces of the gears by means of rigid spiders (RBE2 elements). This modeling approach approximates the bores as infinitely stiff. Other methods could be used for a more accurate description of this boundary surface [23], even though this approach presents the clear advantage of reducing the model complexity, considering also the bulky characteristics of the modeled gears. All the simulations are performed by applying rotational velocity boundary conditions to the *ritzel* gear while the grossrad is left free to rotate around its axis. The model characteristics are summarized in Table 1. It can be seen that the number of nodes for each tooth flank is rather large. This fact would call for the use of many residual attachment modes for each tooth flank. Some eigenmode frequencies are also reported, to give an idea of the frequency range of interest and of the high stiffness of the modeled gears. It will be shown that even for these type of gears, flexibility can play a relevant role and higher importance is expected for more slender

Table 1: Different models used for the numerical simulations

| | **Gear 1: *Ritzel*** | **Gear 2: *Grossrad*** |
|---|---|---|
| **density** $[kg/m^3]$ | 7850 | 7850 |
| **Young's modulus** $[GPa]$ | 210 | 210 |
| **Poisson's ratio** | 0.3 | 0.3 |
| **number of teeth** | 18 | 37 |
| **nodes per flank** | 234 $(9 \times 26)$ | 225 $(9 \times 25)$ |
| **residual attachment modes per flank** | 702 | 675 |
| **total number of nodes** | 103419 | 208270 |
| **total number of elements** | 86064 | 173696 |
| **rigid DOF** | $\theta_x$ | $\theta_x$ |
| **mode 1 frequency** $[kHz]$ | 22.9 | 5.5 |
| **mode 50 frequency** $[kHz]$ | 51.5 | 34.1 |
| **mode 200 frequency** $[kHz]$ | 112.5 | 60.6 |
| **order of magnitude of residual attachment modes frequency** $[kHz]$ | $\cong 350$ | $\cong 300$ |
| **stiffness proportional damping for eigenmodes** | $\cong 10e^{-10}$ | $\cong 10e^{-10}$ |
| **stiffness proportional damping for residual attachment modes** | $\cong 10e^{-7}$ | $\cong 10e^{-7}$ |

gears. The inherent high frequency behavior introduced in the system by the inclusion of the residual attachment modes becomes apparent from Table 1. This fact makes the problem even more numerically stiff and challenging to solve. Special precautions should be taken to avoid spurious behavior. For this reason, when residual attachment modes are introduced, a different value of proportional damping is used for the part that should respond quasi statically. In order to compare the proposed SMS methodology and to study the influence of some parameter solutions with non-linear FE and modally reduced models, several different models have been used as summarized in Table 2.

The non-linear FE model is simulated by using the same mesh as the multibody models and it is composed of linear hexahedral elements. The model accounts for geometric non-linearities and the material law is instead linear. This simulation is performed by using the so-called kinematic contact in Abaqus [24]. This method uses a predictor-corrector algorithm to avoid unphysical penetration. The approach is momentum conserving but not energy conserving, even though for sufficiently fine meshes and small time step sizes, the energy loss can be considered negligible [24]. The integration is carried out with the solver Abaqus/Explicit.

Several modally reduced models are also prepared for comparison. The same FE mesh as for the non-linear FE model is used. The *ritzel* gear is reduced with three different sets of eigenmodes ranging from 20 to 2000, see Table 2. All the eigenmodes are computed using fixed-free boundary conditions, where the bore DOF and so the center of gravity are locked to zero displacement while the teeth flanks are kept free. The *grossrad* gear is reduced with a constant number of 400 fixed-free eigenmodes.

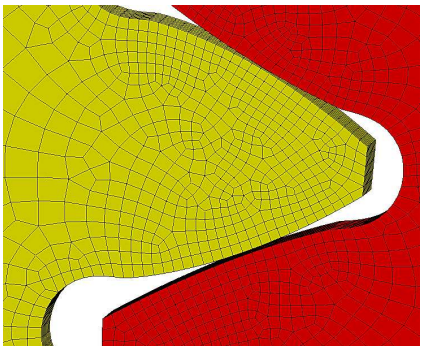

Figure 4: Detail of the gear meshes

Table 2: Different models used for the numerical simulations

| **non-linear FE** | **modal** | | **modal + static augmentation\SMS** | |
|---|---|---|---|---|
| **characteristics** | **id.** | **characteristics** | **id.** | **characteristics** |
| kinematic contact full gear meshes (FEM) $\cong 9 \cdot 10^5$ **DOF** | 20 eig | ***ritzel* gear** 20 eigenmodes ***grossrad* gear** 400 eigenmodes, 420 **flexible DOF** | 50-50 eig + all static | ***ritzel* gear** 50 eigenm.-702 res. att. ***grossrad* gear** 50 eigenm.-675 res. att. 1477 **flexible DOF** |
| | 100 eig | ***ritzel* gear** 100 eigenmodes ***grossrad* gear** 400 eigenmodes 500 **flexible DOF** | 50-100 eig + all static | ***ritzel* gear** 50 eigenm.-702 res. att. ***grossrad* gear** 100 eigenm.-675 res. att. 1527 **flexible DOF** |
| | 2000 eig | ***ritzel* gear** 2000 eigenmodes ***grossrad* gear** 400 eigenmodes 2400 **flexible DOF** | 50-200 eig + all static | ***ritzel* gear** 50 eigenm.-702 res. att. ***grossrad* gear** 200 eigenm.-675 res. att. 1627 **flexible DOF** |
| | | | 50-200 eig + SMS | ***ritzel* gear** 50 eigenm.-var. res. att. ***grossrad* gear** 200 eigenm.-var. res. att. $<$ 400 **flexible DOF** |
| | | | 50-200 eig + SMS teeth | ***ritzel* gear** 50 eigenm.-81 res. att., ***grossrad* gear** 200eigenm.-54 res. att. 250 – 385 **flexible DOF** |
| | | | 100-200 eig + SMS | ***ritzel* gear** 50 eigenm.-var. res. att., ***grossrad* gear** 200 eigenm.-var. res. att. $<$ 450 **flexible DOF** |

Finally, six different models including residual attachment modes are analyzed. In the first three models of Table 2, the gears are reduced with different numbers of fixed-free eigenmodes augmented with 702 residual attachment modes for the *ritzel* gear and 675 for the *grossrad*. This large number is due to the possibility that all the nodes along a tooth flank could go into contact. It has to be noticed that the numbers 702 and 675 are the necessary residual attachment modes to be included when two tooth flanks of a specific teeth pair comes into contact in order to obtain a statically exact solution. Through all the simulations, only the contact between the same two teeth will be simulated, but in case of a full rotation, these numbers should be multiplied by two (the number of flanks) and by the number of teeth, reaching the prohibitively large values of 25272 for the *ritzel* gear and 49950 for the *grossrad* gear. In the particular case of perfectly symmetric gears, symmetry could be exploited. This would allow to use only the full set of residual attachment modes for a single tooth (1404 for the *ritzel* gear and 1350 for the *grossrad*gear). The modal plus static augmentation approach is then only suitable if a small number of teeth impacts are simulated and clearly unfeasible for full gearbox simulations. These models will be used to document the interesting switching behavior of the residual attachment modes, explained in Section 3. In the last three models of Table 2 different static modes switching strategies are implemented. The gears are reduced with fixed numbers of fixed-free eigenmodes while the amount of residual attachment modes is dynamically varied during the simulation following two strategies:

1. **SMS**: In these models, the number of residual attachment modes present in the simulation is varied based on which nodes are detected as in contact by the contact search algorithm. If a certain node is in contact, the corresponding three residual attachment modes for loads in x, y and z direction are included in the reduction. During the so-called free-fly phase in which no teeth are in contact, the dynamic behavior of the gears is accounted for purely by the eigenmodes. The modal participation factors and the initial and final time of activity of each residual attachment mode is then stored for post-processing purposes. In this way, a very small number of residual attachment modes needs to be included in the simulation keeping almost the same accuracy as if the full set of residual attachment modes would be included.
2. **SMS teeth**: In these models, first a fast pre-computation of the contact patch is performed. When time simulation is carried on, the coarse collision detection strategy would detect which teeth are in contact, so that all the residual attachment modes corresponding to the pre-computed contact patch are included simultaneously in the simulation for the full duration of the teeth pair contact and removed after detachment. This approach has the drawback that a pre-computation should be performed and that more residual attachment modes are included at each time step, but presents two major advantages. First the numerical discontinuities that are introduced by the switching strategy might appear only when the first impact is detected and in the teeth pair detachment phase, as opposed to the SMS strategy in which this might happen at each of the time steps in which contact is present. Secondly, the inverse of the mass matrix of the reduced gears can be a priori computed since the size of the reduced model is either equal to the number of eigenmodes or to the number of eigenmodes plus the patch related residual attachment modes. For the case under study the patch size of the *ritzel* gear included 27 nodes and so 81 residual attachment modes, while for the *grossrad* a maximum of only 18 nodes was in contact yielding 54 residual attachment modes.

### *4.2. Time simulation and numerical details*

The equations of motion of the flexible multibody system in Fig.3 are implemented in Matlab in descriptor form and solved by means of an explicit Runge-Kutta scheme of order 4 [18]. For

Table 3: Time simulation details

| | |
|---|---|
| **simulation time** $[ms]$ | $0.2 - 0.3$ |
| **time step size** $[ms]$ | $10e^{-5}$ |
| **penalty factor** $[N/m]$ | $10e^{8} - 2 \cdot 10e^{10}$ |
| **master slave parameter** | $1 - 0.5$ |
| **initial condition *ritzel*** $[rad/s]$ | 5 |
| **initial condition *grossrad*** $[rad/s]$ | 0 |

each different model, the particular sparsity patterns of the resulting mass matrix of the system is exploited. If only eigenmodes are used, the flexible part of the system mass matrix is diagonal, the inversion is trivial and can be performed once, prior to the simulation. When the residual attachment modes are included or the 'SMS teeth' approach is used, the flexible part of the system mass matrix is not diagonal anymore but constant and the inversion can be performed a-priori. When the SMS technique is introduced, the amount of flexible degrees of freedom is substantially reduced but the statically responding part of the mass matrix continuously varies in dimension so that the inversion of this matrix needs to be performed on-line.

The *ritzel* gear starts from an initial rotational velocity of 5 rad/s and one of its teeth hits the *grossrad* gear that on the contrary starts from rest. Only one tooth pair is in contact at each moment in time and the duration of the teeth contact is around 0.12 ms. The numerical simulations details are presented in Table 3.

### *4.3. Influence of eigenmodes, residual attachment modes and penalty factor on the evaluation of contact forces and kinematic quantities*

Given the fact that the modally reduced models were already successfully compared with non-linear FE simulation and experimental results in [18], it is important to underline in which cases modally reduced models should be carefully used. Figure 5 plots the contact forces obtained from several reduced models and shows several interesting phenomena. First of all, it is interesting to notice that, chosing $c_p = 10^8$ N/m to avoid ill-conditioning of the problem, if the number of eigenmodes is increased up to 100, the contact time, notably increases, due to the increasing flexibility of the system. If up to 2000 eigenmodes are included, a sort of convergence can be observed, the solution almost does not vary and the results match the non-linear FE quite accurately. It has to be underlined here, that the eigenmodes up to 2000 have a global nature and still do not include accurate teeth flank local deformation. In the common case in which a non-linear FE reference solution is not present, problems inherent with the penalty formulation and modally reduced flexible bodies may arise. It is in fact possible to notice that if the penalty factor is slightly increased to $c_p = 2.2 \cdot 10^8$ N/m, the solution with 2000 eigenmodes degrades sensibly in accuracy. The contact time is reduced to a value that is comparable more to the unrealistic simulation performed using 20 eigenmodes than to the reference solution. This fact underlines the importance of having a reference simulation when dealing with penalty formulations, and the high sensitivity of the solution to the value of the penalty factor.

Figure 6 highlights instead the behavior of the contact force, when models that include residual attachment modes are adopted. First of all, it is interesting to notice that, when the same penalty factor value $c_p = 10^8$ N/m is used, the model that includes the residual attachment modes shows a large increase in contact time. This fact is expected since the inclusion of the

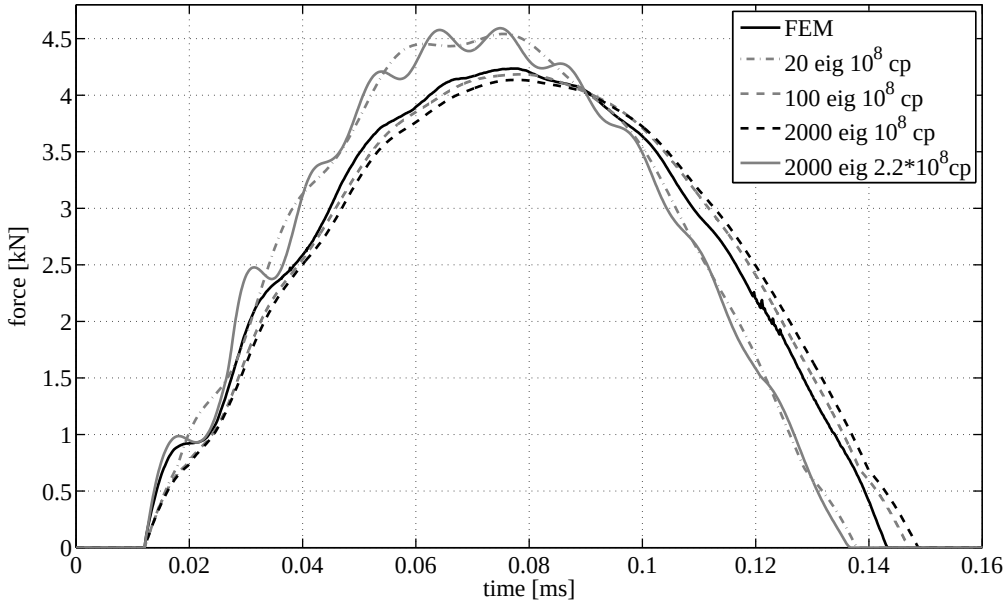


Figure 5: Contact force for different modal reductions

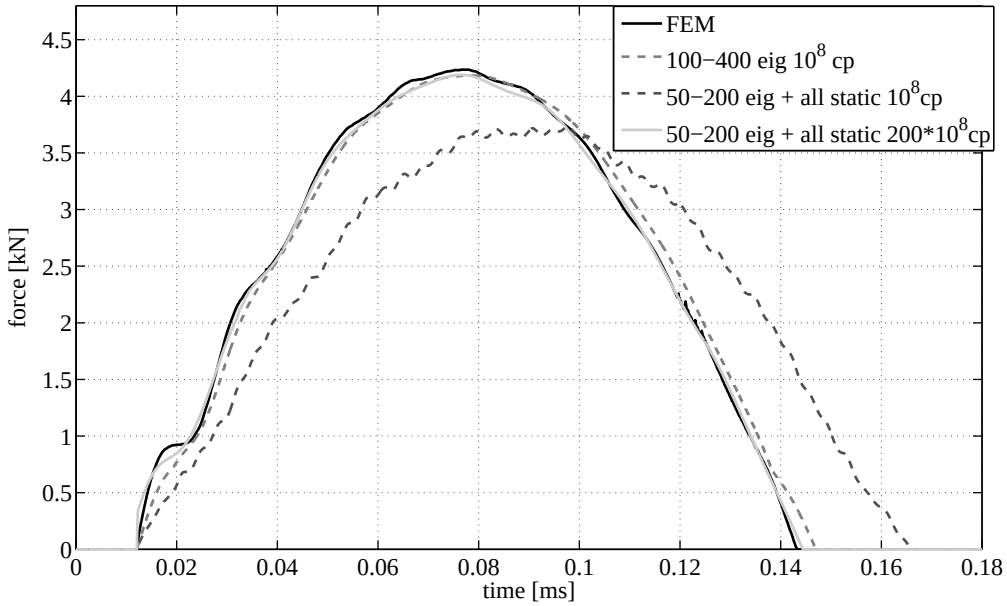


Figure 6: Contact force, compliance induced by residual attachment modes

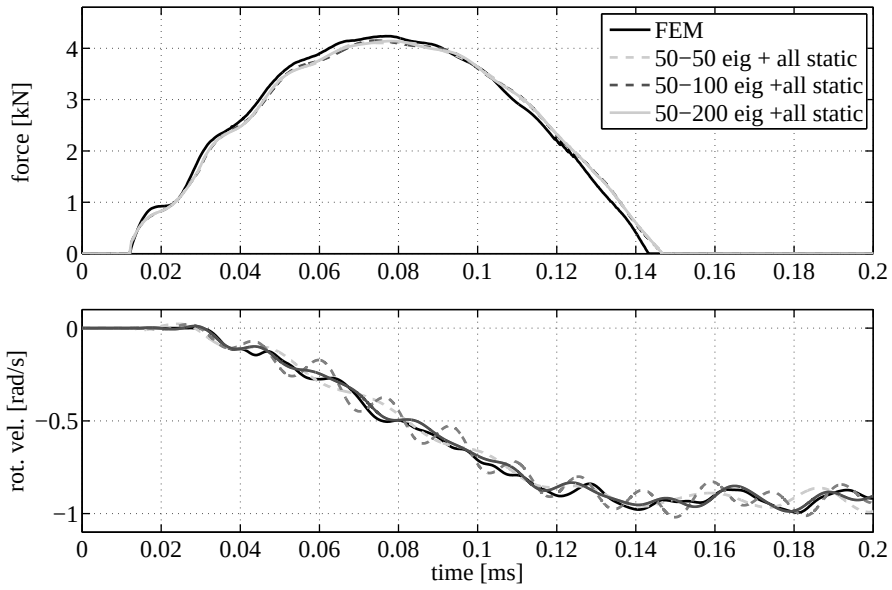


Figure 7: Influence of eigenmodes and residual attachment modes on contact force and rotational velocity

residual attachment modes allows for modeling of the teeth local flexibility. This translates to a lower contact stiffness and a longer contact time. In this case, the penalty factor can be increased with more than two orders of magnitude in order to match closely the non-linear FE contact force. It can be seen that the quality of the simulation including residual attachment modes is high. Another interesting phenomenon is demonstrated Fig.7. The contact force evaluation is only negligibly affected by the amount of eigenmodes included, conversely to the behavior highlighted in Fig.5 and consistently with the fact that the contact force is mainly influenced by the teeth flexibility described by the residual attachment modes. Figure 7 shows though another interesting phenomena. The kinematic quantities, like the depicted rotational velocity of the *grossrad* gear, are instead highly influenced by the amount of eigenmodes included in the reduction, even when the full set of residual attachment modes is included. This fact can also be expected since the dynamic gear behavior is almost entirely accounted for by the eigenmodes. In the free-fly phase, when no contact occurs, after $0.12ms$ the contribution of the residual attachment modes is numerically very close to zero as it will be highlighted in the next sections.

Figure 8 indicates that when these static vectors are included, the solution becomes less sensitive to the value of $c_p$ when sufficiently high. A converging behavior is noticed so that the penalty factor can be increased significantly without a relevant effect on the contact force, until numerical ill-conditioning arises. This behavior was observed multiple times, regardless of the number of eigenmodes included in the simulation. On the contrary, if not enough eigenmodes are included in the simulation, the kinematic quantities like the rotational velocity become largely influenced by the penalty factor value. In Fig.9 a diverging behavior is reported. In fact, during the contact phase, the simulations still give similar results, and instead diverge in the free-fly phase where the dynamic characteristics become of more importance with respect to the local

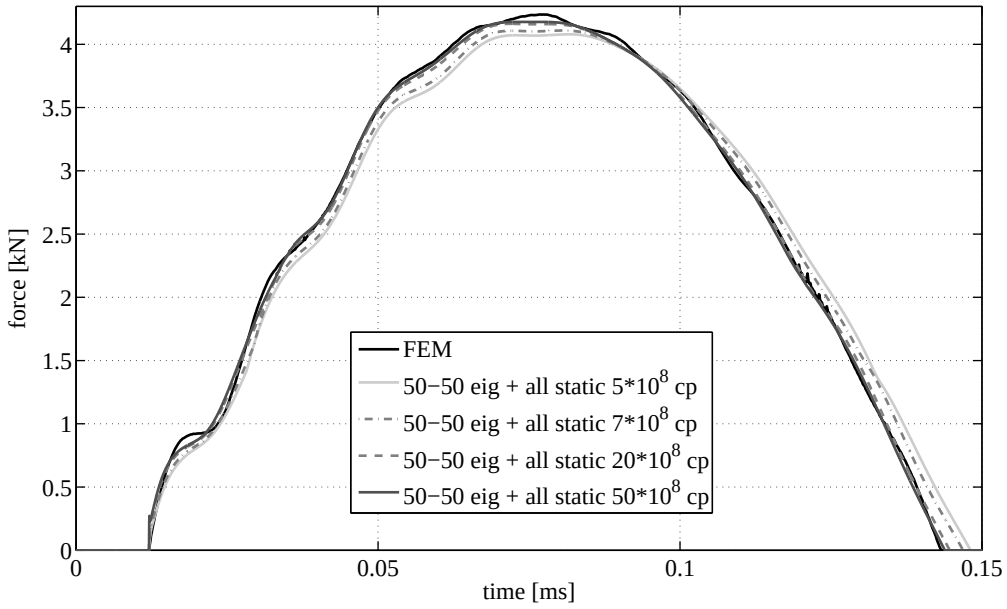


Figure 8: Influence of $c_p$ on contact force: few eigenmodes

flexibility. When an appropriate amount of eigenmodes is included instead, the penalty factor does not play a relevant role anymore if set high enough, see Fig.10.

Given all the previous remarks, it can be stated that the proper inclusion of residual attachment modes might help in the selection of the number of eigenmodes to include in the simulation and the penalty factor value. The following procedure was used in this work. Starting with a relatively low value of the penalty factor, the number of eigenmodes is increased until the rotational velocity does not change significantly anymore. After this step the value of the penalty factor is increased progressively. If the divergence behavior reported in Fig.9 for the kinematic quantities is observed, then the amount of eigenmodes should be increased so that meaningful results could be expected. The amount of eigenmodes should be increased until the penalty factor does not influence the solution anymore as reported in Fig.10.

### *4.4. The switching behavior and different automatic switching strategies for SMS*

It has been shown that the inclusion of residual attachment modes can be useful in different ways for gear contact problems. The main problem that reduces the applicability of this method is the large number of residual attachment modes that should be included in the simulation. One of the main phenomena that should be investigated to asses the possibility of using the SMS idea is, that the modal participation factors related to those residual attachment modes associated with I/O points but that are not lying in the contact region, should not significantly contribute to the system deformation. This behavior is reported in Fig.11 and 12. Here the modal participation factors of four residual attachment modes corresponding to nodes inside the contact region or in its close vicinity are plotted. Particularly, only nodes 17, 18 and 19 are in the contact region. It can be seen that the MPF of the residual attachment mode corresponding to node 16, lying

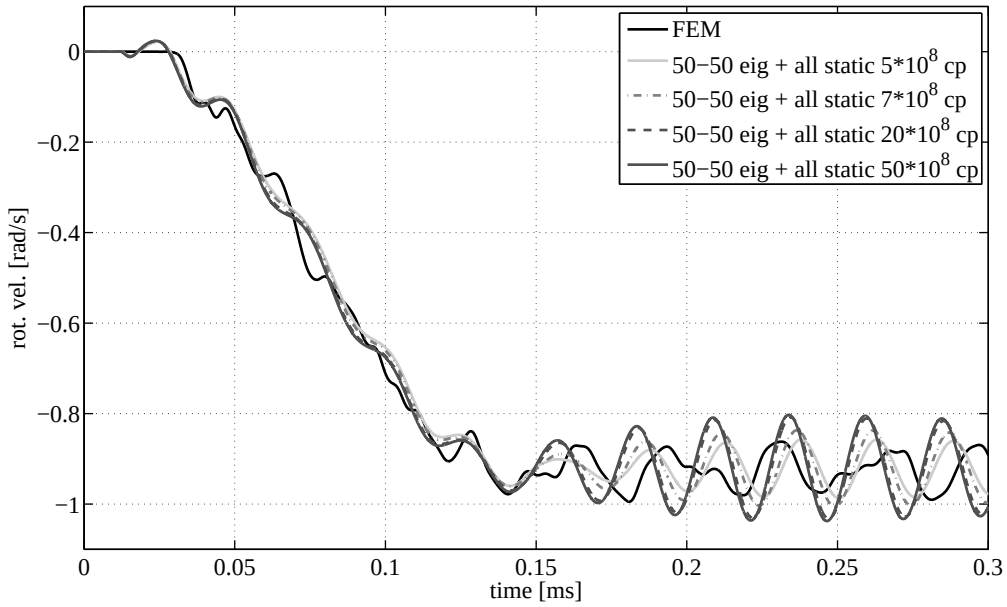


Figure 9: Influence of $c_p$ on rotational velocity of the *grossrad* gear: few eigenmodes

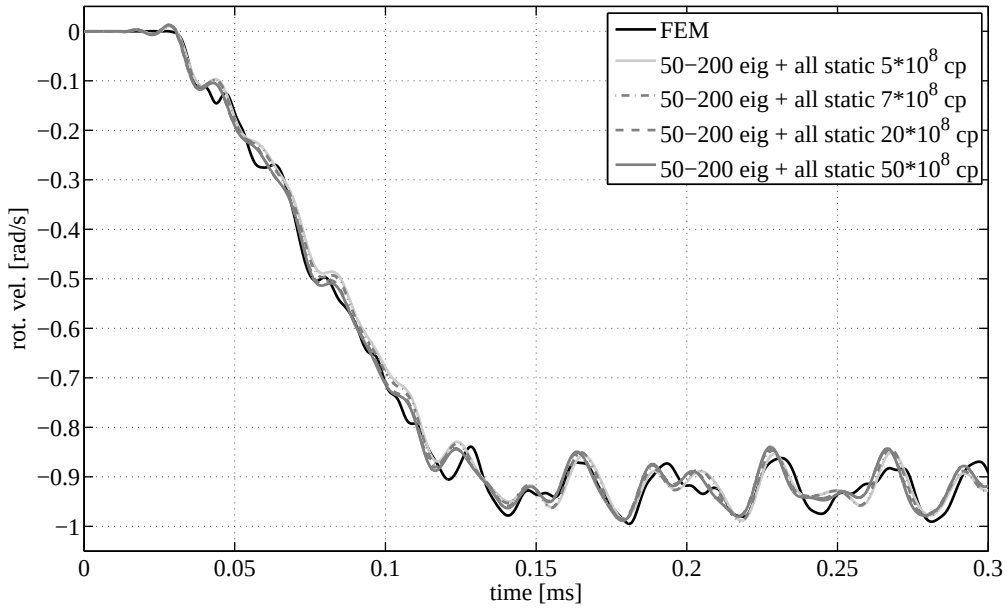


Figure 10: Influence of $c_p$ on rotational velocity of the *grossrad* gear: enough eigenmodes

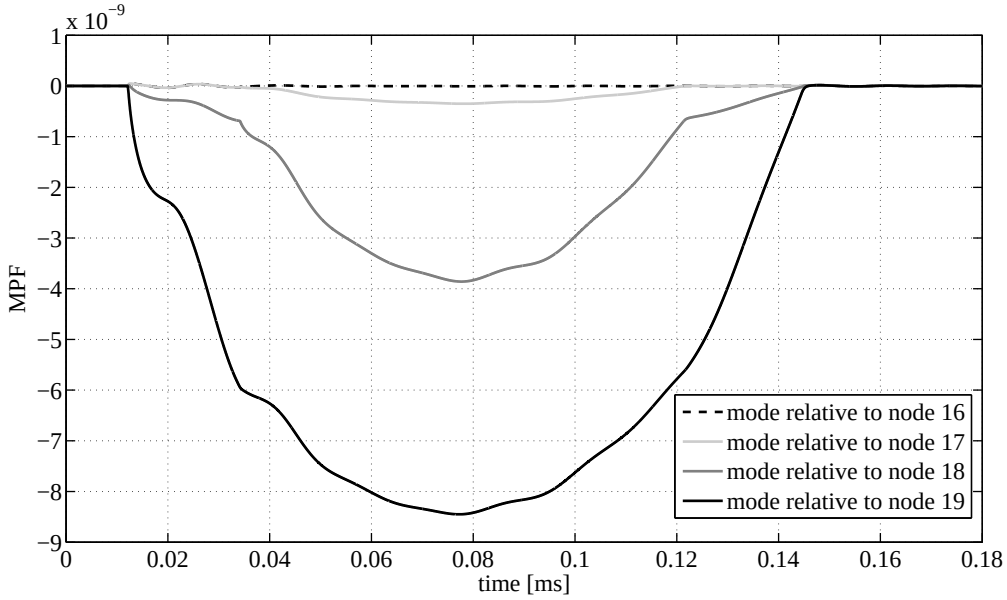


Figure 11: Switching characteristics of residual attachment modes

outside of the contact patch (black dashed line), is some orders of magnitude lower than the others, see Fig.12 . This fact is even more highlighted in the logaritmic scale. All the modes are for obvious reasons equally scaled with respect to the diagonal of the flexile mass matrix. Very interestingly also, the contribution of the residual attachment modes corresponding to nodes in the contact patch damps out very fast after the teeth separation. Given the desirable "switching" behavior of the residual attachment modes, the SMS methodology can be applied. Figure 13 reports several interesting behaviors. First, it can be seen that the SMS solutions are of high quality and they properly match the non-linear FE solution. An improvement with respect to the modally reduced models can be seen, e.g., in the first instants of the contact. Second, regardless which SMS strategy is adopted, the SMS solutions almost overlap to the model that includes all the residual attachment modes without any automatic switching strategy. This fact shows once more, together with Fig.11 that only the active residual attachment modes significantly contribute to the solution. Lastly, as expected, some discontinuities are reported. Around $0.12ms$ after the beginning of the simulation, some impulsive behavior is reported due to the switching strategy. It has to be noted that during the rest of the contact the switching is also active but no numerical discontinuities are observed. This expected numerical issue was solved by using the 'SMS teeth' strategy or by modifying the master-slave parameter. In the first case no impulsive behavior is reported anymore at $0.12ms$ because the switching is active only during the incoming contact and detachment phase. In the second case, by using a value of the master slave parameter $w_f = 0.5$, the numerical discontinuities are properly averaged out. Some very low amplitude oscillations are still observed during the detachment phase. Figure 14 shows instead the rotational velocity of the *grossrad* gear, evaluated using the SMS technique. The matching with the non-linear FE solution is satisfactory. The numerical discontinuities are less pronounced as compared to the

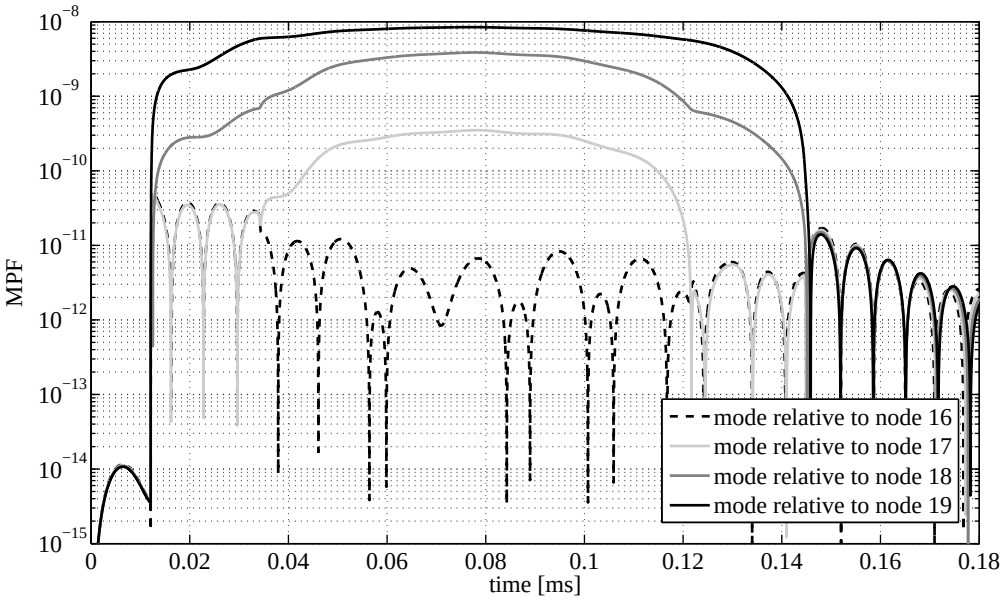


Figure 12: Switching characteristics of residual attachment modes log scale

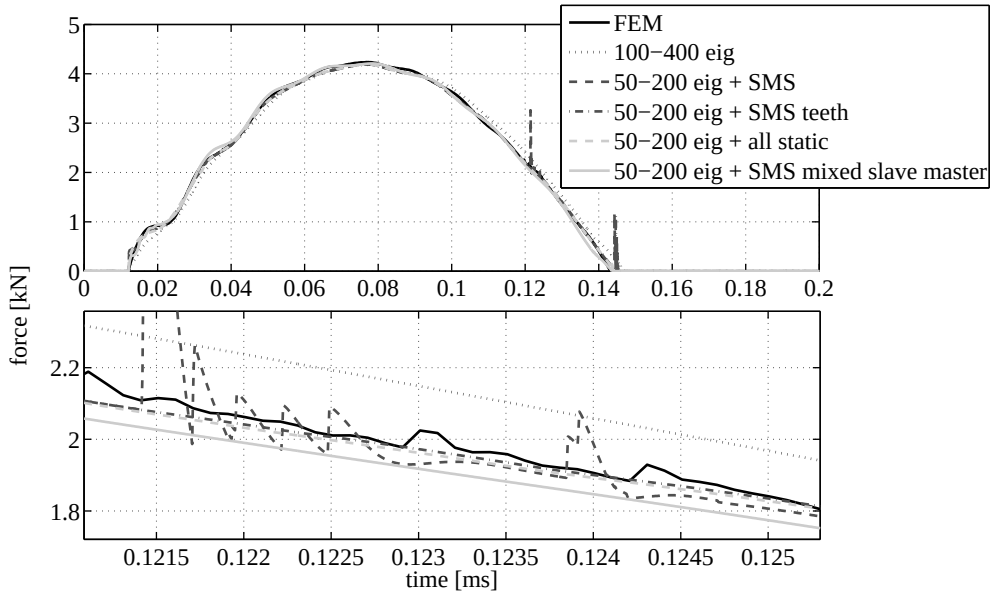


Figure 13: SMS contact force evaluation and discontinuities

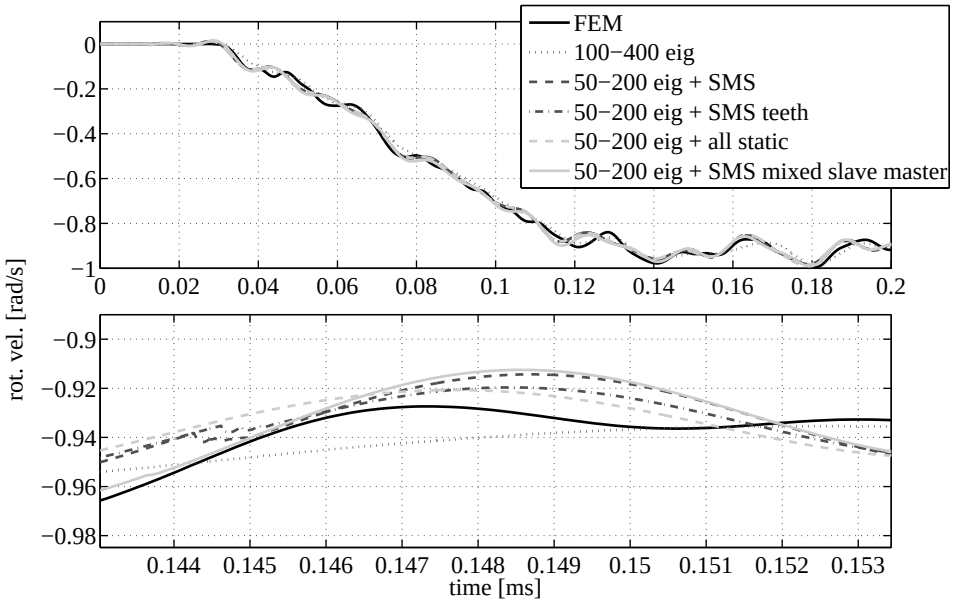


Figure 14: SMS rotational velocity evaluation

contact force evaluation.

The MPF of the eigenmodes, see Fig.15, are computed by using the SMS strategies, without noticeable differences with respect to the models without the switching strategy active. If a MPF factor of an eigenmode that is not significantly excited by the contact forces is plotted, it can be noticed that some discontinuities may arise, see the upper graph of Fig.15. Given the fact that the contribution of these MPF is typically several orders of magnitude lower, as in the plotted case, no influence of this behavior is noticed in the contact force or kinematic quantities, as previously reported.

The behavior of the residual attachment modes is reported in Fig.16. In the top part of the figure, a residual attachment mode that significantly contributes to the local teeth deformation is plotted. The MPF is accurately evaluated by using the SMS strategy. The switching behavior is observed and no numerical discontinuities are reported. The lower part of Fig.16 shows the MPF of a residual attachment mode that is not excited by the contact loads (it is in fact related to an axial load) but is related to a node that lies in the contact patch. The switching behavior is again observed, even though some numerical dicontinuitites and transient behaviors are observed when the SMS strategies are adopted. Given the fact that the contribution of this mode is several orders of magnitude lower as compared to the excited residual attachment modes, this effect has almost no impact on the overall solution. In practice, when it is known that the system will not be excited in a certain direction, the relative residual attachment modes can also be excluded from the simulation. This fact could further reduce the computational burden.

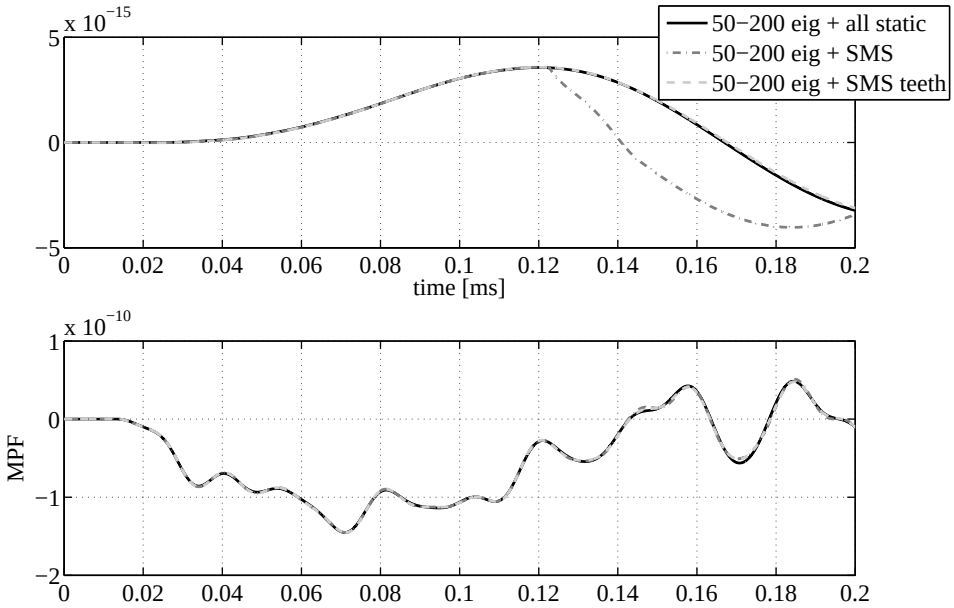


Figure 15: Not excited eigenmode number one and excited eigenmode number three MPF

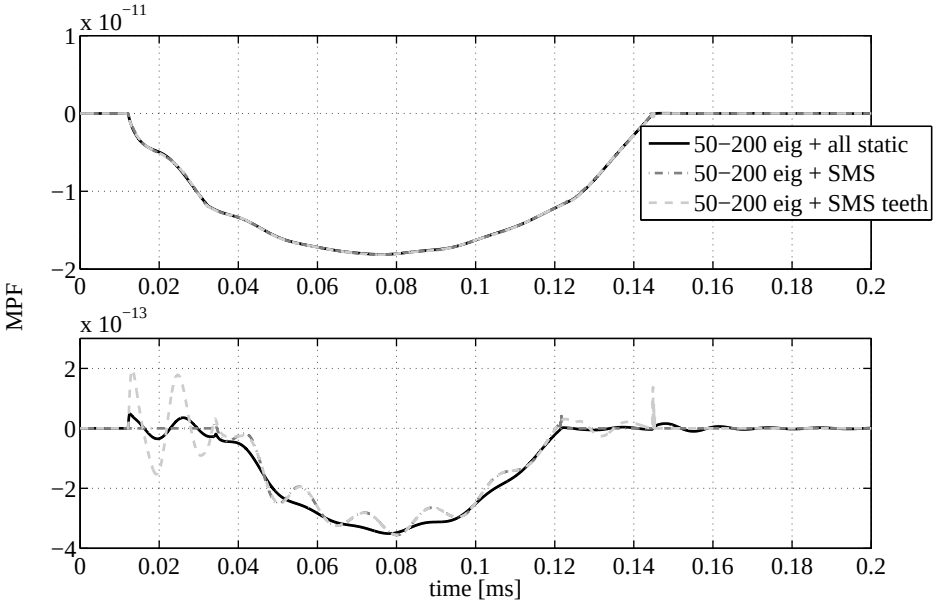


Figure 16: Excited and not excited residual attachment modes MPF

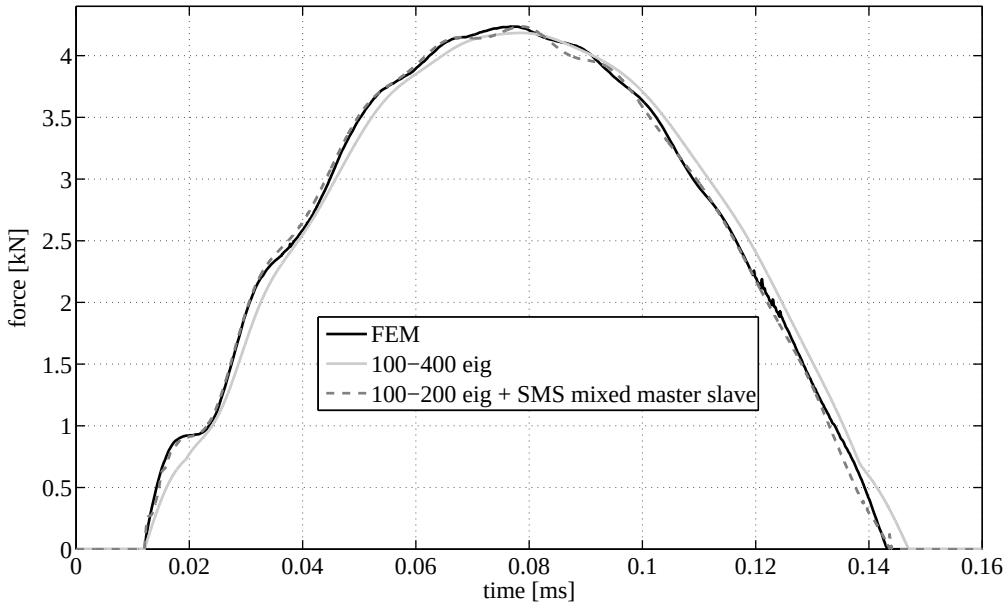


Figure 17: Contact force solution comparison

### *4.5. Final considerations*

Figures 17-18 show a final comparison of the three tested approaches. It can be seen that the SMS methodology is able to replicate the results of the non-linear FE reference simulation accurately and gives more detailed information as compared to modally reduced models. This fact can be noticed both at force level and in the evaluation of the rotational velocities, especially during the contact phase. Moreover, the approach allows for a more physically based selection of the eigenmodes to be included in the simulation and selection of the penalty factor. The computational burden is only slightly reduced with respect to the modally reduced models due to the numerical inversion of the quasi-static part of the flexible mass matrix that need to be perfomed in each time step if SMS is adopted. Techniques for precomputation of this inverse are being explored that could reduce even further the computational time, keeping the same level of accuracy.

## 5. Conclusions

This work discusses how modally reduced flexible multibody models with static augmentation may improve the accuracy of the solution for gear contact modeling. It is shown that the use of residual attachment modes brings many benefits. The amount of eigenmodes and the penalty factor can be chosen in a more physically meaningful way, reducing the need of having computationally expensive reference simulations. This MOR scheme as such cannot be used for systems with variable topology or that present time varying MIMO characteristics as for gear meshing simulations.

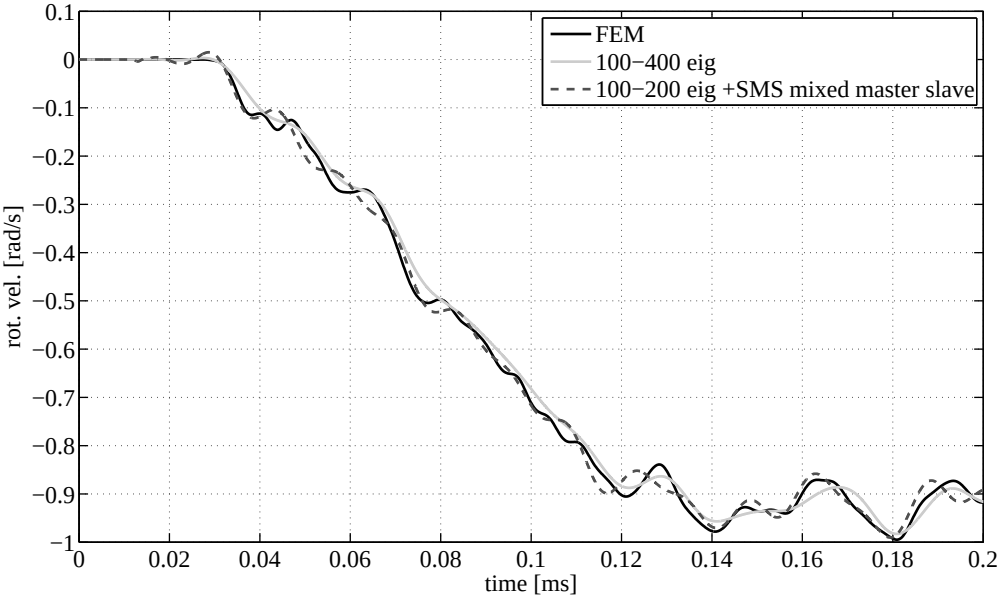


Figure 18: Rotational velocity solution comparison

A methodology named static modes switching has been reviewed and extended in this paper for its use in contact modeling. The method is used for the first time on an example of high complexity and using an explicit integrator that does not present numerical damping. The underlying assumptions of the strategy are numerically tested and a novel automatic switching strategy is implemented purely based on geometrical considerations. Issues related to the numerical discontinuities introduced by the method are discussed and treated consequently. Results show that the method is able to keep the same level of accuracy as if the full modal plus static augmentation is adopted, preserving the higher efficiency of modally reduced models.

Future work will concentrate on improvement of the techniques to reduce the numerical discontinuities, applications to other branches of contact mechanics and further improvement of the numerical efficiency.

## 6. ACKNOWLEDGEMENTS

The European Commission is gratefully acknowledged for the support within the Marie Curie ITN ”VECOM” FP7 - 213543, from which Tommaso Tamarozzi holds an ”Initial Training Grant”

## References

[1] P. Alart, A. Curnier, A mixed formulation for frictional contact problems prone to Newton like solution methods, Computer Methods in Applied Mechanics and Engineering 92 (3) (1991) 353–375.

[2] B. Brogliato, A. Ten Dam, L. Paoli, F. Genot, M. Abadie, Numerical simulation of finite dimensional multibody nonsmooth mechanical systems, Applied Mechanics Reviews 55 (2002) 107.

[3] H. Lankarani, P. Nikravesh, Continuous contact force models for impact analysis in multibody systems, Nonlinear Dynamics 5 (2) (1994) 193–207.
[4] F. Pfeiffer, C. Glocker, Multibody Dynamics with Unilateral Contacts, Wiley, New York, 1996.
[5] S. Vijayakar, A combined surface integral and finite element solution for a three-dimensional contact problem, International Journal for Numerical Methods in Engineering 31 (3) (1991) 525–545.
[6] P. Wriggers, Computational Contact Mechanics, Springer Verlag Berlin, 2006.
[7] P. Ziegler, P. Eberhard, B. Schweizer, Simulation of impacts in geartrains using different approaches, Archive of Applied Mechanics 76 (9) (2006) 537–548.
[8] G. Heirman, T. Tamarozzi, W. Desmet, Static modes switching for more efficient flexible multibody simulation, International Journal for Numerical Methods in Engineering 87 (11) (2011) 1024–1045.
[9] T. Tamarozzi, G. Heirman, W. Desmet, Static modes switching: On-line variable static augmentation for efficient flexible multibody simulation, in: Proceedings of ASME IDETC/CIE 2011, Washington DC, 2011.
[10] P. Flores, M. Machado, M. Silva, J. Martins, On the continuous contact force models for soft materials in multibody dynamics, Multibody System Dynamics 25 (3) (2011) 357–375.
[11] J. Simo, T. Laursen, An augmented Lagrangian treatment of contact problems involving friction, Computers & Structures 42 (1) (1992) 97–116.
[12] F. Auricchio, E. Sacco, Augmented lagrangian finite-elements for plate contact problems, International journal for numerical methods in engineering 39 (24) (1996) 4141–4158.
[13] S. Ebrahimi, A Contribution to Computational Contact Procedures in Flexible Multibody Systems, Dissertation, Schriften aus dem Institut für Technische und Numerische Mechanik der Universität Stuttgart, Shaker Verlag, Aachen, 2007.
[14] V. Ambarisha, R. Parker, Nonlinear dynamics of planetary gears using analytical and finite element models, Journal of Sound and Vibration 302 (3) (2007) 577–595.
[15] A. Shabana, Dynamics of Multibody Systems, Cambridge University Press, Cambridge, 2005.
[16] M. Lehner, P. Eberhard, On the use of moment-matching to build reduced order models in flexible multibody dynamics, Multibody System Dynamics 16 (2) (2006) 191–211.
[17] R. Schwertassek, O. Wallrapp, A. Shabana, Flexible multibody simulation and choice of shape functions, Nonlinear Dynamics 20 (4) (1999) 361–380.
[18] P. Ziegler, Dynamische Simulation von Zahnradkontakten mit elastischen Modellen, Dissertation, Schriften aus dem Institut für Technische und Numerische Mechanik der Universität Stuttgart, Volume 23, Shaker Verlag, Aachen, 2012.
[19] R. Craig, A review of time-domain and frequency-domain component mode synthesis methods, Journal of Modal Analysis 2 (2) (1987) 59–72.
[20] J. Fehr, Automated Error Controlled Model Reduction in Elastic Multibody Systems, Dissertation, Schriften aus dem Institut für Technische und Numerische Mechanik der Universität Stuttgart, Volume 21, Shaker Verlag, Aachen, 2011.
[21] Z. Zhong, Finite Element Procedures for Contact-Impact Problems, Oxford University Press Oxford, 1993.
[22] P. Ziegler, P. Eberhard, Simulative and experimental investigation of impacts on gear wheels, Computer Methods in Applied Mechanics and Engineering 197 (51) (2008) 4653–4662.
[23] G. Heirman, W. Desmet, Interface reduction of flexible bodies for efficient modeling of body flexibility in multibody dynamics, Multibody System Dynamics 24 (2) (2010) 219–234.
[24] Dassault Systémes, Abaqus theory manual (2009).

# Static modes switching in gear contact simulation

T. Tamarozzi[a,*], P. Ziegler, P. Eberhard[b], W. Desmet[a]

[a]*Department of Mechanical Engineering, KU Leuven, Celestijnenlaan 300B, 3001 Heverlee (Leuven), Belgium*
[b]*Institute of Engineering and Computational Mechanics, University of Stuttgart, Pfaffenwaldring 9, 70569 Stuttgart, Germany*

**Abstract**

Contact modeling is an active research area in the field of multibody dynamics. Despite the important research effort, two main challenging issues, namely accuracy and speed, are not yet jointly solved. One main issue remains the lack of model order reduction schemes capable to efficiently treat systems where multiple, a priori unknown, input-output locations are present. This work first analyzes the importance of including the necessary residual attachment modes by numerical simulation of two gears meshing in an ad-hoc flexible multibody model. Given the large number of residual attachment modes needed, the methodology named static modes switching is extended and successfully applied to improve efficiency. The method proposes an on line selection of residual attachment modes for accurate local deformation prediction. The applicability to impact problems is discussed through numerical experiments and the automatic selection strategy is based purely on geometrical information. Results show that the method can be applied to gear meshing simulation, obtaining a high level of accuracy while preserving computational efficiency. Comparisons are made between modally reduced models, full non-linear finite element and the proposed strategy

*Keywords:* static modes switching, gear contact, impact, flexible multibody dynamics, model reduction, static augmentation

## 1. Introduction

Contact modeling is a very active research area in the field of multibody (MB) dynamics. Despite a large number of papers and books, e.g. [1–6] describing in detail different contact methodologies for continuous contacts and impacts, two of the main challenging issues, namely accuracy and speed, are far from being jointly solved. Industrial needs call for lighter and more powerful machines, in which the flexibility of the components has to be addressed, especially when contact and impact are involved as, e.g., for gear meshing in drivelines [7]. In this context, faster and more accurate simulation might be necessary to obtain the correct kinematics and reaction load distribution, but also stresses and strains, extending the model validity towards durability related quantities.

*Corresponding Author: Tommaso Tamarozzi, Dept. Mechanical Engineering, KU Leuven, Celestijnenlaan 300B, 3001 Heverlee (Leuven), Belgium, Tel.: +32 16 328608, Fax +32 16 322987
*Email address:* tommaso.tamarozzi@mech.kuleuven.be (T. Tamarozzi )

Contact and more specifically gear train simulations are theoretically and numerically very challenging problems. When they are dealt with by using flexible MB techniques, the contact formulation adopted and the model used to represent body flexibility plays a dominant role. Accurate and efficient ways of incorporating the highly dynamic effects related to contacts and impacts need to be coupled with Model Order Reduction (MOR) techniques that are particularly challenged by the multiple input-output (MIMO) nature of the problem. With the intention to extend the methodology named Static Modes Switching (SMS) presented in [8] and [9] to different branches of contact mechanics, this work discusses how SMS can be adapted for efficient and accurate contact simulation in case of complex geometries and in the presence of impacts as it occurs during gear meshing simulation. The SMS methodology adapts during simulation the mode set used to represent component flexibility by judiciously choosing only those residual attachment modes that are contributing actively to the body deformation. This technique is particularly useful when simulating mechanisms in which loading is possible in many degrees of freedom (DOF), but only few of them are simultaneously loaded at a given moment in time.

The outline of the present work is as follows. In Section 2 the state of the art of contact modeling schemes and MOR techniques is briefly summarized, highlighting the main advantages and disadvantages. In Section 3 the particular penalty formulation adopted is revised in more details and the theory behind the SMS idea is discussed. Section 4 describes the gear model used and the details of the performed numerical experiments. Results are shown that clearly highlight the positive influence of the use of residual attachment modes on the evaluation of the force and local teeth deformation. It is also documented how the proposed MOR approach allows for an easier selection of the number of eigenmodes to be included and how the penalty factor can be sensibly increased until convergence of relevant kinematic quantities. The SMS idea is then adopted in different variants to allow for efficient computation, maintaing the high level of accuracy typical of more complex models. All results are compared against a reference nonlinear Finite Element (FE) simulation. Finally some conclusions are presented summarizing the main contributions of the paper and highlighting further extensions of the method and remaining open issues.

## 2. Review of contact modeling and model order reduction techniques

### *2.1. Contact modeling in flexible multibody simulation*

In the last decades, a large variety of contact formulations in an MB framework has been proposed in literature. Without claim of completeness, it is possible to summarize the most frequently used approaches in the following categories:

1. **Compliant continuous force model**: In this approach, usually referred to as penalty approach, see e.g. [3, 10], the contact between rigid bodies is described by continuous force functions that account for local flexibility effects like non-linear material dependency including energy dissipation, geometric effects and kinematic influences. The majority of these models are based on the well known Hertz theory and are described by means of non-linear power functions that are mainly influenced by the stiffness of the contacting bodies and the coefficient of restitution. The main advantages lie in its simplicity, ease of implementation, stability of the integration and high numerical efficiency. The major drawback is the difficult selection of the proper force law parameters. Moreover, the assumption of rigid bodies might not be justified especially when wave propagation effects play an important role. Numerically expensive reference simulations are usually needed to validate the model.